Cell. Mol. Biol. (ISSN: 1165-158X)

Journal Homepage: www.cellmolbiol.org

Cellular and Molecular Biology

Original Article

Effect of peniocerol on human meniscal fibrochondrocyte inflammation induced by IL-1β and TNF-α through the NF-κB signaling pathway

Brandon Eduardo Galicia-Canales[1,2], María del Rocío Aguilar-Gaytán[2#], Marco Antonio Álvarez-Pérez[3], Katia Jarquín-Yáñez[4], Beatriz del Carmen Couder-Garcia[5], Mariano Martínez-Vázquez[6], Alexandra Berenice Luna-Angulo[7], Laura Sánchez-Chapul[7], Olivia Hernández-González[8], Monica Adelaida Saldaña-García[9], David Hernández-Velasco[10], Carlos Landa-Solís[1,2*]

[1] Posgrado en Ciencias Biológicas, Universidad Nacional Autónoma de México, México City 04510, México
[2] Cellular Therapy and Regenerative Medicine Tissue Engineering Unit, Instituto Nacional de Rehabilitación Luis Guillermo Ibarra Ibarra, Mexico City 14389, Mexico
[3] Tissue Bioengineering Laboratory, DEPeI-FO, National Autonomous University of Mexico, Circuito Exterior s/n, Ciudad Universitaria, Ciudad de México 04510, Mexico
[4] Laboratory of Immunotherapy and Tissue Engineering, Department of Cellular and Tissue Biology, Faculty of Medicine, National Autonomous University of Mexico (UNAM), Av. Universidad 3000, Copilco Universidad, Coyoacán, Ciudad de México 04510, Mexico
[5] SECIHTI-Centro de Investigación y Asistencia en Tecnología y Diseño del Estado de Jalisco, Subsede Sureste, Parque Científico Tecnológico de Yucatán, Tablaje Catastral 31264, Mérida 97302, México
[6] Instituto de Química, Universidad Nacional Autónoma de México, C. Exterior, C. Universitaria, Coyoacán, 04510, CDMX México
[7] Laboratory of Neuromuscular Diseases, Division of Clinical Neurosciences, Instituto Nacional de Rehabilitación Luis Guillermo Ibarra Ibarra, Mexico City 14389, Mexico
[8] Laboratorio de Microscopía Electrónica, Instituto Nacional de Rehabilitación Luis Guillermo Ibarra Ibarra, Mexico City 14389, Mexico
[9] Banco de sangre, Instituto Nacional de Rehabilitación Luis Guillermo Ibarra Ibarra, Mexico City 14389, Mexico
[10] Instituto Tecnológico y de Estudios Superiores de Monterrey, Mexico City 14380, Mexico

Article Info

Article history:

Received: November 14, 2025
Accepted: February 03, 2026
Published: March 31, 2026

Use your device to scan and read the article online

Abstract

It is currently known that meniscal damage has a bidirectional relationship with the onset/development of osteoarthritis (OA), making the development of new therapeutic strategies that comprehensively address both issues crucial. In this context, the present study aimed to evaluate the biological effect of peniocerol (PEN), an emerging phytopharmaceutical, in an in vitro model of inflammation induced by IL-1β and TNF-α in human meniscal fibrochondrocyte cells. Human meniscal fibrochondrocyte cells were isolated, cultured, and treated with different concentrations of PEN to determine those that promote cell proliferation and the IC_{50} using the MTT assay. The cells were then stimulated with TNF-α (10 ng/mL) or IL-1β (5 ng/mL), with or without PEN (300 and 500 µM). Cell morphology and the expression of ACAN, type I+III collagen, type II collagen, MMP13, and p65 were evaluated by immunofluorescence. Treatment with TNF-α and IL-1β significantly reduced the expression of ACAN and type II collagen, while increasing MMP13 and p65, indicating a degenerative phenotype. Co-treatment with PEN at 300 µM showed partial improvements, while PEN at 500 µM normalized the levels of ACAN, Col2A1, and p65 to values similar to the control, while significantly inhibiting the markers for COL I+III and MMP3. In an in vitro degenerative fibrochondrocyte model, PEN at 500 µM demonstrated its ability to halt extracellular matrix degradation and actively promote its recovery, showing an optimal balance between efficacy and safety as a potential therapeutic strategy for the comprehensive treatment of OA progression.

Keywords: Meniscal fibrochondrocyte cells, Osteoarthritis, Peniocerol, Phytopharmaceuticals, Proinflammatory cytokines.

1. Introduction

Osteoarthritis (OA) is one of the most common degenerative joint diseases worldwide, affecting more than 25% of the global population [1]. OA affects all structures of the knee joint, including articular cartilage, subchondral bone, the synovial membrane, ligaments, and the menis-

∗ Corresponding author.
E-mail address: clanda@inr.gob.mx (C. Landa-Solís).
# These authors contributed equally
Doi: http://dx.doi.org/10.14715/cmb/2025.72.3.5

cus [2–4]. In recent years, the meniscus has gained relevance and has become a focal point in studies regarding the initiation/progression of knee OA [5]. The meniscus's limited blood supply results in a poor healing capacity following injury, causing many injuries and age-associated degeneration to be permanent [6]. The loss of its cushioning function leads to joint instability, increasing stress on the articular cartilage and subchondral bone [7], thus accelerating the development of osteoarthritis [8,9].

At the cellular level, the meniscus is composed of two cell populations: a fusiform population located on the surface and an ovoid or polygonal population in the rest of the meniscus. These cells, when cultured *in vitro*, are referred to as fibrochondrocyte cells [10,11]. Furthermore, it has been described that inflammatory responses secondary to articular cartilage degeneration affect the meniscal cellular microenvironment [12,13]. It has been proposed that when the extracellular matrix (ECM) is degraded or suffers structural damage, it releases damage-associated molecular patterns (DAMPs) that initiate inflammatory responses [14,15]. Immune cells can detect DAMP signals, migrate to the damaged meniscus, and produce pro-inflammatory cytokines and chemokines such as IL-1β, IL-6, or TNF-α [16–21]. This inflammation, in turn, may increase the expression of catabolic enzymes of the extracellular matrix, stimulate blood vessel proliferation, and promote further immune infiltration into the meniscal tissue, ultimately leading to the loss of homeostasis within the joint microenvironment [22]. In the specific case of fibrochondrocyte cells exposed to IL-1β, it has been reported that the expression of collagen types I, II, III, and VI genes (COL1A1, COL2A1, COL3A1, COL6A1) and aggrecan (ACAN) are downregulated, while genes involved in matrix degradation (MMP1, MMP3, MMP13, and ADAMTS5) are upregulated [23–25].

Recent reports indicate that meniscal damage has a bidirectional relationship with the onset of OA, highlighting the importance of addressing both issues comprehensively in joint health management and treatment [26]. In this context, recent research has emphasized the ability of natural products to generate anti-inflammatory effects without causing significant adverse side effects. Therefore, we have decided to focus our investigation on peniocerol (PEN), a sterol isolated from the root of *Myrtillocactus geometrizans* [27]. Initially, PEN showed cytotoxic activity in some human tumor cell lines [28]. Furthermore, various studies have documented the anti-inflammatory and antihyperalgesic effects of PEN, which have fueled our interest in this molecule. In these studies, using both *in vitro* and *in vivo* inflammation models in rats, it has been demonstrated that PEN effectively inhibits inflammation induced by carrageenan in the rat paw, reducing both edema and hyperalgesia in a dose-dependent manner. This compound exhibited activity comparable to that of ketorolac, a well-known non-steroidal anti-inflammatory drug (NSAID). Similarly, PEN displays marked anti-inflammatory activity by reducing myeloperoxidase (MPO) enzyme activity in inflamed tissue, a key marker of inflammation. In the inflammation model induced by 13-acetate of 12-O-tetradecanoylphorbol (TPA) in mouse ears, it inhibited edema in a dose-dependent manner, with ED_{50} values equal to or lower than those of indomethacin [27]. Moreover, in the edema model induced by ethyl phenylpropiolate (EPP), PEN showed inhibition comparable to that of dexamethasone, suggesting a potential effect on the production of prostaglandins and other inflammatory mediators through a steroidal pathway [27].

Based on the findings described for PEN, the objective of the present study was to analyze the biological effect of PEN on inflammation induced by IL-1β and TNF-α in isolated human meniscal cells *in vitro*. This will generate basic knowledge that, in future research, may help clarify whether PEN has the potential to be a candidate for the development of new alternative therapies for the treatment of OA.

2. Materials and methods

2.1. Isolation and culture of fibrochondrocytes

Human meniscal samples were obtained from remnants of partial or total meniscectomies, with prior informed consent from the patients. The procedure was conducted in accordance with the Ethical Code of the World Medical Association (Declaration of Helsinki) and was approved by the Research Committee of the "Luis Guillermo Ibarra Ibarra" National Institute of Rehabilitation in Mexico (Ref. 09/09). The meniscal remnants were received in the operating room, placed, and transported in phosphate-buffered saline (PBS) solution with 10% antibiotic-antimycotic (PBS/50mL tube, all from Gibco, Life Technologies, Carlsbad, CA, USA). In the laboratory, within a Class II laminar flow hood, the PBS was removed, and the tissue was placed in a 60 mm Petri dish with enough DMEM-F12 culture medium (Gibco, Life Technologies, Carlsbad, CA, USA) to keep it hydrated. Using a scalpel (No. 21), the tissue was processed into approximately 1 mm^2 fragments, after which the tissue was transferred to a 50 mL tube with 10 mL of DMEM-F12 culture medium containing 0.2% Type II collagenase (Worthington, Lakewood, NJ, USA). The tube was placed in an orbital shaker (150 rpm) at 37°C for 3–4 hours. Subsequently, the cells released from the extracellular matrix were collected by centrifugation at 300 G for 10 minutes. To expand the initial cell number, the cells were transferred to culture flasks (75 cm^2) and incubated at 37°C, 5% CO2, for the necessary time to reach 80%–90% confluence, with medium changes every two days (DMEM/F12 with 10% Fetal Bovine Serum (FBS) and 1% antibiotics-antimycotics, all from Gibco, Life Technologies, Carlsbad, CA, USA). To collect the cells, 0.25% trypsin-EDTA (Gibco, Life Technologies, Carlsbad, CA, USA) was used, and the cells were stored in aliquots of 1×10^6 cells/mL in cryovials, which were kept submerged in liquid nitrogen at -196°C until experimental use.

2.2. Peniocerol preparation

The compound peniocerol (3β, 6α-diol-cholest-8-ene) was isolated from *Myrtillocactus geometrizans* and purified according to the methodology previously reported by Salazar et al., 2011 [27]. We worked with an aliquot of the compound used by Couder et al., 2019 [29], and the primary stock solution (4.13 mM) was kept at -20 ºC and prepared in DMSO (Sigma-Aldrich, St. Louis, MO, USA).

2.3. Cytotoxicity assays by peniocerol

To document the cytotoxic effect on isolated meniscal fibrochondrocyte cells, 15×10^3 cells per well were seeded in 96-well plates in triplicate, allowing cell attachment by incubating (37°C, 5% CO2, DMEM/F12 culture medium

with 10% FBS and 1% antibiotics-antimycotics) for 24 hours prior to exposure to the peniocerol concentrations (control without treatment, 100 µM, 200 µM, 300 µM, 400 µM, 500 µM, 600 µM, 700 µM, 800 µM, and 900 µM). These concentrations were added in place of the culture medium and incubated for 24 hours. Afterward, the culture medium was removed and replaced with culture medium containing 5 µL of MTT reagent (Sigma-Aldrich, Darmstadt, Germany), and the cells were incubated for 4 hours. Finally, the absorbance of each well was quantified in a plate reader equipped with a 490 nm filter (DTX 800, Beckman Coulter, Indianapolis, IN, USA). To determine the IC50, the absorbance of the control was compared with that of the treated wells.

2.4. Effect of peniocerol on fibrochondrocytes treated with IL-1β and TNF-α

To assess the effect of peniocerol on fibrochondrocyte cells exposed to IL-1β and TNF-α, 1×10^5 cells were seeded on 18 mm diameter coverslips, which were cultured in 12-well culture plates in DMEM/F12 with 10% FBS and 1% antibiotics-antimycotics at 37°C, 5% CO2. Twenty-four hours after the initial seeding, the treatment scheme was initiated in triplicate: control (no treatment), IL-1β (5 ng/mL, Invitrogen, Waltham, MA, USA), IL-1β + peniocerol 300 µM, IL-1β + peniocerol 500 µM, TNF-α (10 ng/mL, Invitrogen, Waltham, MA, USA), TNF-α + peniocerol 300 µM, TNF-α + peniocerol 500 µM, for 24 hours. This experiment was first performed to evaluate changes in morphology and proteoglycan expression by toluidine blue staining, followed by quantification. The same experiment was repeated for analysis by immunofluorescence of the expression of meniscal tissue-specific proteins and proteins involved in the inflammation process within the knee joint.

2.5. Changes in morphology and proteoglycan expression

At the end of the treatment, the culture medium was removed, and the cells were washed twice with phosphate-buffered saline (PBS, pH 7.4). Fixation was carried out with 4% formaldehyde for 15 minutes at room temperature, followed by another wash with PBS. The cells were then incubated with a 0.05% toluidine blue solution prepared in 0.1 M acetic acid (pH approximately 4.0) for 30 minutes at room temperature. After staining, the coverslips were washed with distilled water to remove excess dye and were allowed to air dry completely.

For quantification of the bound dye, the toluidine blue was extracted by incubating each coverslip in absolute ethanol for 30 minutes with gentle agitation at room temperature. Subsequently, 100 µL of the extracted solution from each sample was transferred to a 96-well plate for spectrophotometric reading. Absorbance was measured at 630 nm using a DTX 800 plate reader (Beckman Coulter, Indianapolis, IN, USA). The absorbance values were corrected with the corresponding blanks and expressed as relative absorbance or percentage compared to the control group.

2.6. Immunofluorescence analysis

At the end of the treatments, cells cultured on coverslips were washed with PBS and fixed with 4% formaldehyde for 15 minutes at room temperature. Subsequently, they were permeabilized with 0.1% Triton X-100 for 10 minutes and blocked with a 5% bovine serum albumin (BSA) solution in PBS for 1 hour at room temperature to prevent nonspecific antibody binding. The coverslips were then incubated overnight at 4°C with primary antibodies diluted in PBS with 1% BSA: monoclonal anti-Aggrecan antibody (Santa Cruz®, cat. sc-33695), monoclonal anti-MMP-13 antibody (Santa Cruz®, cat. sc-515284), polyclonal anti-collagen type III antibody (Abcam®, cat. ab7778), monoclonal anti-p65 antibody (Santa Cruz®, cat. sc-8008), and polyclonal anti-collagen type II antibody (Abcam®, cat. ab34712). After incubation, the cells were carefully washed with PBS and incubated for 1 hour at room temperature with the corresponding secondary antibodies, all diluted 1:1000: anti-mouse IgG conjugated to FITC (Thermo Scientific®, cat. F-2761), anti-rabbit IgG conjugated to FITC (Abcam®, cat. ab6717), and anti-mouse IgG2a conjugated to Alexa Fluor® 594 (Abcam®, cat. ab150120). After washing with PBS to remove excess secondary antibody, the coverslips were mounted onto slides using a mounting medium with DAPI for nuclear staining.

Images were captured using a Carl Zeiss® Axio Imager A1 fluorescence microscope, using specific filters according to the fluorochrome employed, and processed for quantitative analysis of fluorescence intensity using ImageJ® software (NIH, National Institutes of Health, Bethesda, MD, USA). The same exposure, threshold, and analysis parameters were applied to all samples to ensure comparability between treatments.

2.7. Statistical analysis

All experiments were performed at least three times independently. Data are expressed as mean ± standard deviation (SD). Statistical analyses were performed using GraphPad Prism software with Student's t-test, one-way ANOVA, or two-way ANOVA; $p < 0.05$ and $p < 0.01$ were considered statistically significant.

3. Results

3.1. Evaluation of the half inhibitory concentration (IC50)

The MTT assay was used to detect the toxic effects of different concentrations (0 to 1,000 µM) of PEN on fibrochondrocyte cells. The IC50 was determined, and concentrations of PEN lower than 1491 µM did not affect cell

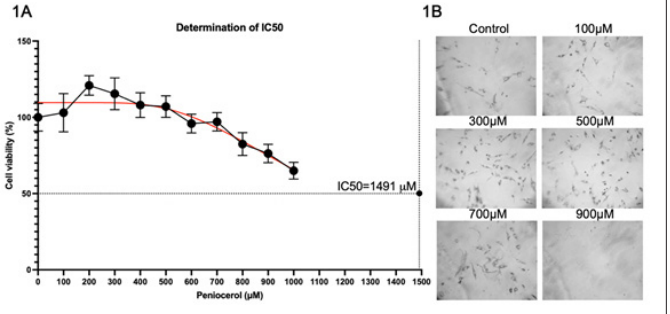


Fig. 1. Cell viability and morphological assessment in response to PEN treatment. A. Cell viability percentage at different PEN concentrations evaluated by the MTT assay read at 490 nm. The IC50 was determined to be 1491 µM. The results are presented as mean ± standard deviation. B. The images show the cellular morphology at each concentration, compared with the control group.

viability. Figure 1A shows the dose-dependent decrease in cell viability, with an increase in viability at doses between 100 and 500 µM. As a result, concentrations of 300 and 500 µM of PEN were selected for subsequent experiments. Figure 1B shows micrographs of cells treated with different concentrations of PEN, compared to the control group. A progressive decrease in cell viability is observed as the PEN concentration increases, as evidenced by the cell morphology.

3.2. Changes in morphology and proteoglycan expression

To determine the changes in the synthesis or retention of extracellular matrix (ECM) components, toluidine blue staining was applied, followed by spectrophotometric quantification at 620 nm in cells treated with IL-1β and combinations with different concentrations of the PEN compound. In the obtained micrographs (Figure 2A, left), less intense staining is observed in the group treated only with IL-1β, suggesting a decrease in the proteoglycan-rich extracellular matrix. In contrast, the groups co-treated with PEN300 and PEN500 showed a progressive increase in staining intensity, highlighting an apparent recovery of the ECM content, particularly in the IL-1β + PEN500 group.

The quantitative analysis (Figure 2B, right) confirmed these observations. Treatment with IL-1β induced a significant decrease in absorbance at 620 nm compared to the control group ($p < 0.05$), indicating a loss of extracellular matrix. Co-administration with PEN at 300 µM showed partial recovery without reaching statistical significance compared to the control, while the 500 µM concentration restored absorbance levels significantly above the IL-1β group ($p < 0.01$) and reached values higher than the control ($p < 0.05$), suggesting a protective or restorative effect of the compound on the ECM degraded by IL-1β.

Representative micrographs (Figure 3A, left) show a lower staining intensity in the TNF-α-treated group, suggesting a decrease in the amount of deposited proteoglycans. In comparison, the co-treated groups with PEN show a progressive recovery of ECM content, with more intense staining, particularly in the TNF-α + PEN500 group.

The quantitative analysis of absorbance at 620 nm (Figure 3B, right) confirmed these observations. The TNF-α-treated group showed a significant decrease in absorbance compared to the control group ($p < 0.01$), indicating a loss of extracellular matrix. Co-treatment with PEN300 resulted in partial recovery ($p < 0.05$ vs. TNF-α), while the 500 µM concentration showed significant restoration of ECM levels compared to TNF-α ($p < 0.001$) and reached values higher than the control group ($p < 0.05$).

These results suggest that treatment with TNF-α compromises the integrity of the extracellular matrix and that the compound PEN, particularly at 500 µM, has a protective or restorative effect on the ECM affected by the induced inflammation.

Finally, the micrographs (Figure 4A, left) show the distribution of ECM and cell organization at different PEN concentrations compared to the control. In the PEN300-treated group, the cells show somewhat less intense staining, but with a more compact and organized arrangement than in the control group. In the PEN500-treated group, a greater amount of ECM is observed, with significantly more intense staining and a dense and organized cell distribution, suggesting an effective increase in ECM.

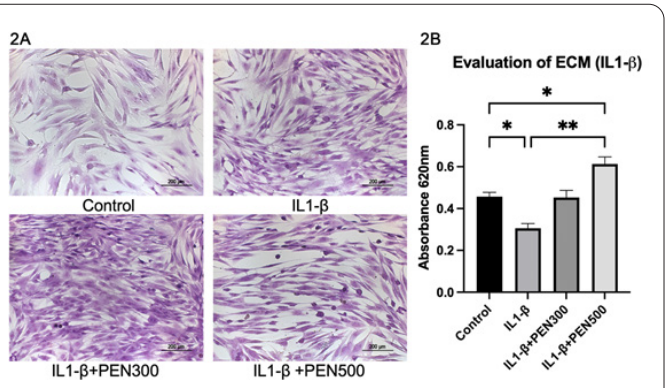


Fig. 2. Morphological evaluation and extracellular matrix quantification in IL-1β-treated fibrochondrocyte cells exposed to PEN. A. Morphological evaluation and extracellular matrix (ECM) quantification in cells treated with IL-1β and PEN. Micrographs show Toluidine blue staining, highlighting morphological alterations induced by IL-1β and progressive recovery with PEN (300 and 500 µM). Control cells exhibit typical fibroblastic morphology and parallel organization, while IL-1β induces thinning and cellular disorganization. PEN500 partially restores morphology and staining. B. The graph represents absorbance at 620 nm of Toluidine blue, as an indirect measure of ECM content. Data are presented as mean ± SD. *p < 0.05, **p < 0.01. Scale bar: 200 µm, 20X.

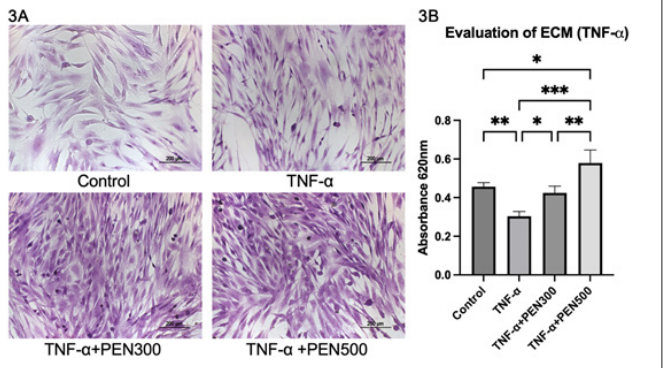


Fig. 3. Morphological evaluation and extracellular matrix quantification in TNF-α -treated fibrochondrocyte cells exposed to PEN. A. Morphological evaluation and extracellular matrix (ECM) quantification in cells treated with TNF-α and PEN. Micrographs show Toluidine blue staining; TNF-α induces evident morphological alterations such as disorganization and reduced cell density, while co-administration with PEN (300 and 500 µM) promotes recovery of fibroblastic morphology and staining associated with ECM. B. The graph represents absorbance at 620 nm of Toluidine blue, as an indirect measure of ECM content. Data are presented as mean ± SD. *p < 0.05, **p < 0.01, ***p < 0.001. Scale bar: 200 µm, 20X.

The quantitative analysis of absorbance at 620 nm (Figure 4B, right) reveals that the PEN300-treated group has higher absorbance compared to the control group ($p < 0.01$), promoting a similar recovery of the ECM.

These results indicate that PEN, at a concentration of 300 µM, has a restorative effect on the extracellular matrix, as evidenced by the increase in toluidine blue absorbance and the improvement in cell organization. However, no significant difference was observed between the control and PEN500 groups, suggesting that the 300 µM dose is sufficient for this effect on the extracellular matrix.

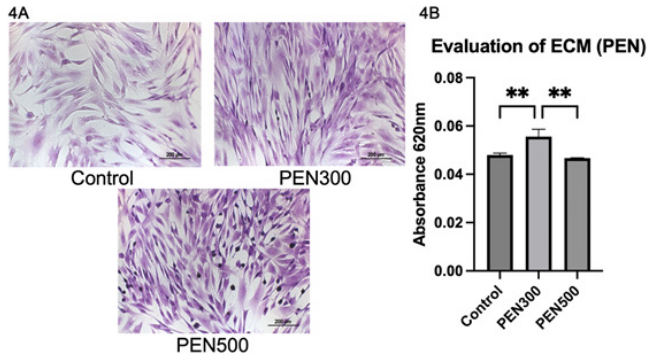


Fig. 4. Cell morphology and extracellular matrix content in fibrochondrocyte cells treated with PEN. A. Morphological evaluation and extracellular matrix (ECM) quantification after PEN treatment. Micrographs show Toluidine blue staining; control group cells exhibit typical fibroblastic morphology with an organized structure. In the PEN-treated groups, a progressive restoration of cell density and morphological organization is observed, with the most pronounced effect in the PEN500 group. B. The graph represents absorbance at 620 nm of Toluidine blue, as an indirect measure of ECM content. Data are presented as mean ± SD. **p < 0.01. Scale bar: 200 µm, 20X.

3.3. Immunofluorescence analysis

The results revealed significant changes in the expression of key extracellular matrix proteins and inflammatory markers under different experimental conditions, demonstrating the adverse effects induced by pro-inflammatory cytokines as well as the protective action of peniocerol (PEN).

First, the expression of aggrecan (ACAN), a proteoglycan essential for the structure and function of hyaline cartilage, was studied. In the untreated (control group) condition, fibrochondrocyte cells exhibited abundant ACAN expression. However, when the cells were exposed to TNF-α (10 ng/mL) or IL-1β (5 ng/mL), a notable decrease in fluorescence intensity for ACAN was observed (Figures 5A and 5B, respectively; $p < 0.05$ and $p < 0.0001$). This reduction was particularly evident at the cell periphery, suggesting an alteration in extracellular matrix secretion and deposition. Adjunctive treatment with PEN showed a dose-dependent effect: while at 300 µM a partial recovery of the signal was observed, at 500 µM the fluorescence intensity of ACAN reached levels comparable to the control ($p < 0.001$ for PEN300 and $p < 0.01$ for PEN500 vs TNF-α-treated group, and $p < 0.0001$ for PEN300 and PEN500 vs IL-1β-treated group), indicating nearly complete restoration of proteoglycan synthesis (see Figures 5A and 5B).

The co-expression of type I and type III collagen, components of the extracellular matrix, was evaluated alongside MMP13, a key metalloproteinase in cartilage degradation. The analysis revealed a pattern similar to that described for ACAN, with pro-inflammatory cytokines inducing a marked increase in the expression of type I and III collagen (Figures 5C for TNF-α and 5D for IL-1β; $p < 0.01$), with a fluorescent signal distribution suggesting a reorganization of the cytoskeleton towards a more fibrotic phenotype. Simultaneously, a strong signal for MMP13 was detected ($p < 0.01$), a metalloproteinase that exhibited a peri-nuclear and vesicular localization pattern, consis-

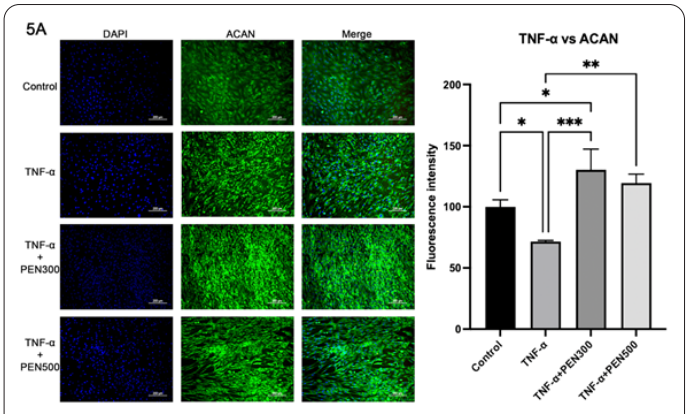


Fig. 5A. ACAN expression in fibrochondrocyte cells treated with TNF-α and PEN. ACAN (green) expression in human fibrocartilage cells. From left to right in the graph: Control without treatment shows an intense cytoplasmic signal. Treatment with TNF-α (10 ng/mL) markedly reduces fluorescence (*p < 0.05). Co-treatment with PEN (300 and 500 µM) restores the ACAN signal in a dose-dependent manner (***p < 0.001 and **p < 0.01 vs TNF-α). Nuclei stained with DAPI (blue). Scale bar: 200 µm, 20X.

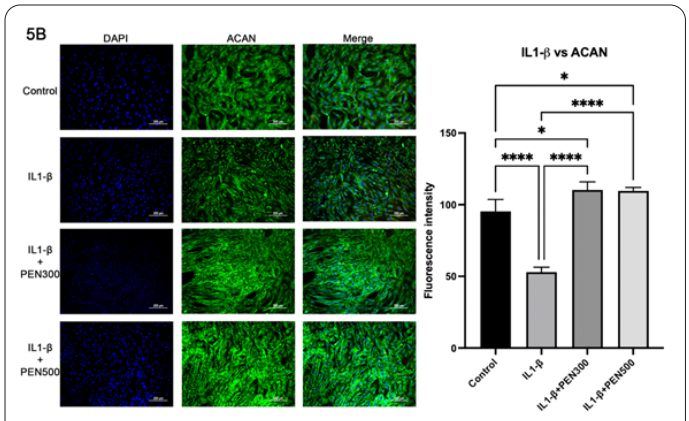


Fig. 5B. ACAN expression in fibrochondrocyte cells treated with IL-1β and PEN. Effect of IL-1β (5 ng/mL) on ACAN (green). From left to right in the graph: Control. IL-1β significantly decreases expression (****p < 0.0001). PEN (300 and 500 µM) recovers ACAN levels (****p < 0.0001 vs IL-1β). Scale bar: 200 µm, 20X.

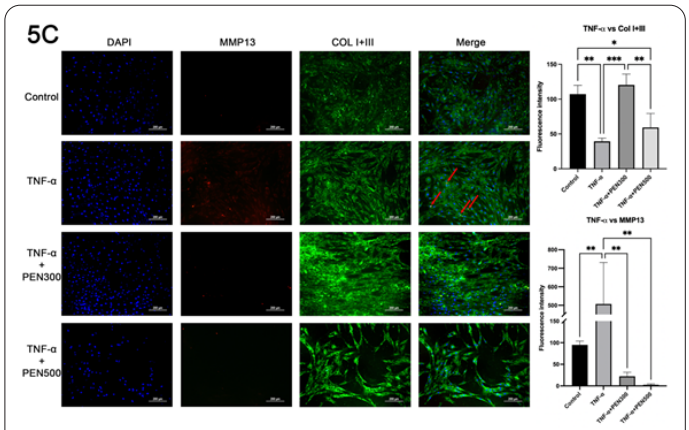


Fig. 5C. Collagen I+III and MMP13 expression in fibrochondrocyte cells treated with TNF-α and PEN. Immunofluorescence for collagen I+III (green) and MMP13 (red) in fibrocartilage cells treated with TNF-α and exposed to PEN. Analysis of collagen I+III (green) and MMP13 (red) expression after TNF-α treatment. From left to right in the upper graph (Col I and III): Control shows low basal expression, co-treatment with peniocerol at 300 µM decreases collagen I+III expression (**p < 0.01). From left to right in the lower graph (MMP13): TNF-α induces a significant increase in MMP13 expression (**p < 0.01), and co-treatment with PEN (300 µM and 500 µM) reduces MMP13 expression (**p < 0.01). Red arrows: peri-nuclear localization of MMP13. Scale bar: 200 µm, 20X.

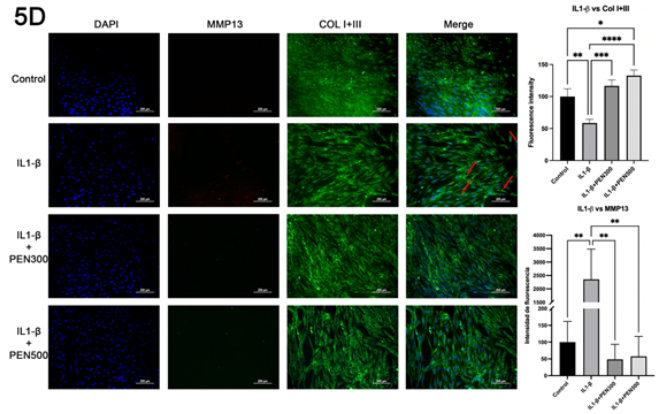


Fig. 5D. Collagen I+III and MMP13 expression in fibrochondrocyte cells treated with IL-1β and PEN. Immunofluorescence for collagen I+III (green) and MMP13 (red) in fibrocartilage cells treated with IL-1β and exposed to peniocerol. From left to right in the upper graph (Col I and III): IL-1β alone decreases Col I and III expression (**p < 0.01), followed by co-treatment with PEN 300 μM, which increases collagen I+III (***p < 0.001), and PEN 500 μM, which also increases collagen I+III (****p < 0.001). From left to right in the lower graph (MMP13), IL-1β induces a significant increase in MMP13 expression compared to the untreated control (**p < 0.01), while PEN (300/500 μM) normalizes its expression (**p < 0.01). Red arrows: MMP13 vesicles. Scale bar: 200 μm, 20X.

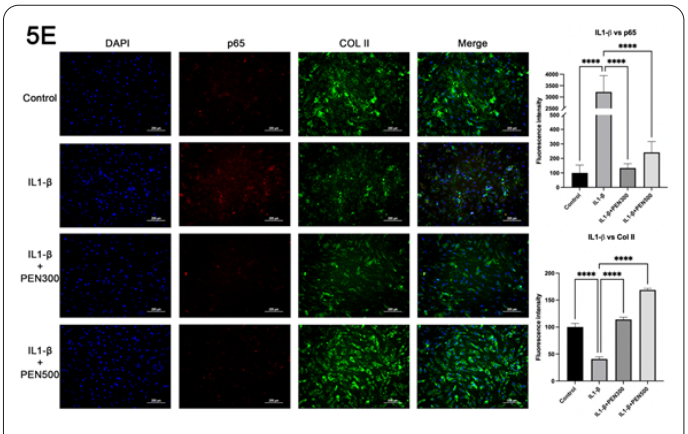


Fig. 5E. COL2A1 and p65 expression in fibrochondrocyte cells treated with IL-1β and PEN. Immunofluorescence for collagen II (COL2A1, green) and p65 (red) in fibrocartilage cells treated with IL-1β and exposed to peniocerol. From left to right in the upper graph (p65): IL-1β activates the overexpression of p65 compared to the control (****p < 0.001), and treatment with PEN (300/500 μM) returns p65 levels to values very similar to the control, while showing a significant difference against the IL-1β-treated group (****p < 0.001). From left to right in the lower graph (Collagen type II): IL-1β significantly inhibited (****p < 0.001) the expression of COL2A1 compared to untreated fibrocartilage cells, and co-treatment with PEN at 300/500 μM significantly increased (****p < 0.001) the expression of COL2A1 compared to the untreated control. Scale bar: 200 μm, 20X.

tent with its activation and secretion. Adjunctive treatment with PEN significantly reduced both the expression of fibrotic collagens and MMP13, with this effect being more pronounced at 500 μM, where the signal for these markers decreased by more than 60% compared to the groups treated with cytokines alone (see Figures 5C and 5D).

Finally, the expression of type II collagen, the main component of hyaline cartilage and present in smaller proportions in the meniscus, was analyzed alongside p65, a key nuclear component of the NF-κB transcription complex involved in the inflammatory response. Under control group conditions, strong expression of type II collagen and minimal nuclear presence of p65 were observed. After exposure to IL-1β (Figure 5E) or TNF-α (Figure 5F), a significant decrease in type II collagen and intense activation of p65 were observed, reflecting the loss of a chondrogenic phenotype transitioning towards a fibrotic one, alongside the activation of inflammatory pathways. The administration of peniocerol significantly attenuated the effects induced by both IL-1β and TNF-α, reducing the activation of p65, with the nuclear signal decreasing by more than 70% compared to the cytokine-only groups, and in contrast, type II collagen expression was recovered, especially at 500 μM. Additionally, statistical analyses confirmed these differences with significant values ranging from $p < 0.01$ to $p < 0.001$..

Taken together, these results demonstrate that peniocerol can effectively counteract the negative effects of TNF-α and IL-1β on human fibrochondrocytes by preserving the expression of structural components of the meniscus and inhibiting both matrix degradation and the activation of inflammatory pathways (see Figures 5A–F).

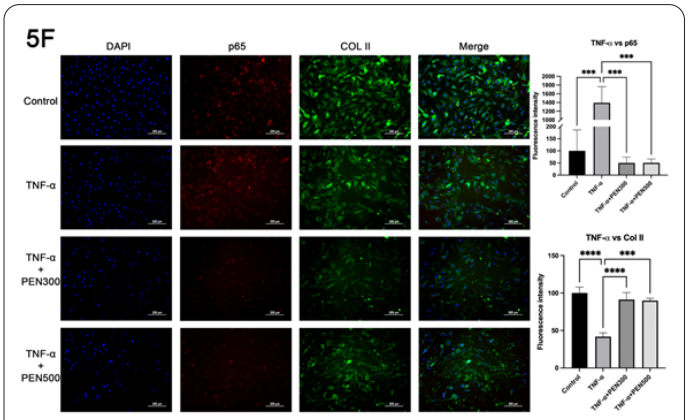


Fig. 5E. COL2A1 and p65 expression in fibrochondrocyte cells treated with TNF-α and PEN. Immunofluorescence for collagen II (COL2A1, green) and p65 (red) in chondrocytes treated with TNF-α. From left to right in the upper graph (p65): Similar to IL-1β, TNF-α activates the overexpression of p65, and also similar to what was described for IL-1β, PEN concentrations (300/500 μM) inhibited the induction of p65 by TNF-α, showing a statistically significant decrease compared to the group that received only TNF-α (***p < 0.01). From left to right in the lower graph (Collagen type II): Similarly to IL-1β, treatment with TNF-α decreases the expression of COL2A1 compared to the untreated control (****p < 0.001), and co-treatment with PEN at 300/500 μM normalizes the expression of COL2A1, with no statistically significant differences compared to the untreated control, and in contrast, showing a significantly elevated expression (****p < 0.001 and ***p < 0.01) compared to the group that received only TNF-α. Scale bar: 200 μm, 20X.

4. Discussion

One of the first results of this research was the determination of the IC50 of PEN on human meniscal fibrochondrocyte cells: 1491 μM. In a previous study, the cytotoxicity of PEN was analyzed in colon cancer cell lines: SW-620 (IC50 = 48.8 μM), HCT-15 (IC50 = 39.1 μM), and HCT-116 (IC50 = 47.7 μM)[29], indicating that PEN is selectively cytotoxic against malignant cells compared to cells from healthy tissue. This can be attributed to the

Warburg effect, according to which tumor cells, characterized by an accelerated metabolism and elevated baseline levels of oxidative stress, are more susceptible to compounds that generate additional oxidative stress, disrupt mitochondrial function, or cause DNA damage[30,31].

Continuing with the analysis of the cytotoxicity curve of PEN on fibrochondrocyte cells (see Figure 1), it was observed that from a concentration of 120 to 500 μM, PEN exhibited a positive effect on cellular metabolism compared to the untreated control. Based on this finding, we decided to use concentrations of 300 and 500 μM of PEN to evaluate the effect of this molecule in an inflammation model induced by IL-1β or TNF-α in human meniscal fibrochondrocyte cells *in vitro*.

One of the initial findings was the inhibition of NF-κB with a potential anti-inflammatory effect. This effect was observed at a concentration of 300 μM, and more notably at 500 μM, which significantly reduced the nuclear signal of p65 (>70%), restoring levels comparable to the untreated group (inflammation, see Figures 5E and 5F). Our results can be compared with those reported for a flavonoid isolated from honey, called chrysin, which significantly blocks the degradation of IκB-α and the activation of NF-κB in isolated human hyaline cartilage chondrocytes exposed to IL-1β [30–32]. These findings support the classification of PEN as a nutraceutical fitting into the profile of NF-κB inhibitors, with potential as an anti-inflammatory modulator for the meniscus.

Another significant discovery in our research was the evidence of extracellular matrix (ECM) recovery. At a concentration of 300 μM, the recovery was partial, while at 500 μM of PEN, a complete restoration, or even enhancement over the control group, was observed. This was reflected both in the staining intensity (Toluidine blue) and cellular organization (see Figures 2 and 3, panels A and B). Similarly, this concentration (PEN 500 μM) induced a full restoration of ACAN (see Figures 5A and 5B), COL I/III (see Figures 5C and 5D), and COL2A1 (see Figures 5E and 5F) to levels comparable to the untreated control. Similar results have been reported in *in vivo* rabbit models, where in an inflammation model (via IL-1β), a gel based on the Wnt5a growth factor and platelet-rich plasma (PRP) was applied, resulting in the protection of the ECM in the meniscal cells of rabbits receiving the treatment [33,34]. Additionally, in an ovine model of meniscal damage repair using a hydroxyapatite (HA) scaffold and stem cells, the use of this therapeutic strategy led to an increase in proteoglycans, collagen I/II, and a reduction in MMP-13 and IL-1β expression in the treated menisci [35]. Based on our findings, PEN has the potential to be applied in *in vivo* animal models for meniscal matrix reconstruction, as demonstrated in other experimental treatment strategies.

It is noteworthy that at the 500 μM dose of PEN, it actively participated in our inflammation model, regulating MMP-13 and the homeostasis of collagen I/III (elevated by TNF-α and IL-1β). After treatment, a significant reduction in MMP-13 (>60%) was observed, a value similar to that obtained in the untreated control (see Figures 5C and 5D), as well as a significant recovery of collagen types I and III, indicating the reversal of the fibrotic phenotype of the cells induced by the inflammation model. Finally, the restoration of basal COL2A1 levels was observed, indicating that PEN favors the restoration of extracellular matrix (ECM) homeostasis (see Figures 5E and 5F). Furthermore, our results align with previous studies that have reported that when NF-κB is activated by inflammatory cytokines such as IL-1β and/or TNF-α, MMP-13 is overexpressed, resulting in the loss of collagen homeostasis in the knee microenvironment affected by osteoarthritis (OA) [36,37]. This leads us to hypothesize that PEN, at a concentration of 500 μM, not only participates in inhibiting inflammation but also in maintaining the matrix architecture of the fibrochondrocyte cells treated with this compound.

Finally, it is important to highlight the dose-dependent effect of PEN at 300 μM, which was partial, in contrast to the 500 μM dose, which was complete and similar to the control values not exposed to TNF-α and IL-1β. This is consistent with reports for flavonoids such as chrysin, which require specific doses for the regulation of IκB-α and NF-κB [38], or astaxanthin, which has also been reported to require specific doses for its protective action in the ECM of chondrocytes [39].

According to our results, PEN could have the same potential described for other natural-origin immunomodulators such as astaxanthin [39], resveratrol [40,41], and chrysin [42,43], which have shown promising results in inflammatory models of the knee joint environment. Undoubtedly, the knowledge generated by this work can be used to continue investigating PEN as an immunomodulator and ECM regenerating agent in future animal models and preclinical studies.

The 500 μM concentration of PEN applied in a cytokine-induced degeneration model in isolated human meniscal fibrochondrocyte cells in vitro demonstrated the ability of this molecule to restore the ECM in the treated cells by normalizing the proteins ACAN, COL I, III, and COL2A1, followed by the restoration of cellular morphology (inhibition of MMP-3). At the same time, the expression of p65 was normalized, indicating the regulation of the NF-κB signaling pathway with the subsequent anti-inflammatory effect.

Abbreviations

ACAN: Aggrecan, BSA: Bovine Serum Albumin, COL I: Collagen type I, COL II / COL2A1: Collagen type II, COL III: Collagen type III, CO_2: Carbon dioxide, DAMPs: Damage-Associated Molecular Patterns, DMEM/F12: Dulbecco's Modified Eagle Medium/Ham's F-12, DMSO: Dimethyl sulfoxide, ECM: Extracellular matrix, ED_{50}: Median effective dose, EPP: Ethyl phenylpropiolate, FBS: Fetal bovine serum, FITC: Fluorescein isothiocyanate, IC_{50}: Half maximal inhibitory concentration, IL-1β: Interleukin-1 beta, IL-6: Interleukin-6, MMP: Matrix metalloproteinase, MMP13: Matrix metalloproteinase-13, MPO: Myeloperoxidase, MTT: 3-(4,5-dimethylthiazol-2-yl)-2,5-diphenyltetrazolium bromide, NF-κB: Nuclear factor kappa-light-chain-enhancer of activated B cells, NSAID: Non-steroidal anti-inflammatory drug, OA: Osteoarthritis, PBS: Phosphate-buffered saline, PEN: Peniocerol, PRP: Platelet-rich plasma, SD: Standard deviation, TNF-α: Tumor necrosis factor alpha, TPA: 12-O-tetradecanoylphorbol-13-acetate.

Conflict of interest

All authors declare no conflicts of interest.

Consent for publication

All authors have read and approved the final manuscript

for publication.

Acknowledgments
This paper was submitted in partial fulfillment of the requirements for the MSc degree in the Master's Program in Biological Sciences at UNAM. We thank Ingrid Salgado Gutiérrez for her help in preparing the material required for the development of the study.

Author contributions
The authors contributed equally.

Funding
None.

Ethics approval
The procedure was conducted in accordance with the Ethical Code of the World Medical Association (Declaration of Helsinki) and was approved by the Research Committee of the "Luis Guillermo Ibarra Ibarra" National Institute of Rehabilitation in Mexico (Ref. 09/09).

References

1. Chen D et al (2017) Osteoarthritis: toward a comprehensive understanding of pathological mechanism. Bone Res 5:16044
2. Marchev AS et al (2017) Oxidative stress and chronic inflammation in osteoarthritis: can NRF2 counteract these partners in crime? Ann NY Acad Sci 1401(1):114–135
3. Latourte A, Kloppenburg M, Richette P (2020) Emerging pharmaceutical therapies for osteoarthritis. Nat Rev Rheumatol 16:673–688
4. Kraus VB, Blanco FJ, Englund M, Karsdal MA, Lohmander LS (2015) Call for standardized definitions of osteoarthritis and risk stratification for clinical trials and clinical use. Osteoarthritis Cartilage 23:1233–1241
5. Driban JB et al (2019) Accelerated Knee Osteoarthritis Is Characterized by Destabilizing Meniscal Tears and Preradiographic Structural Disease Burden. Arthritis Rheumatol 71:1089–1100
6. Felson DT (2010) Arthroscopy as a treatment for knee osteoarthritis. Best Pract Res Clin Rheumatol 24(1):47–50
7. Fukubayashi T, Kurosawa H (1980) The Contact Area and Pressure Distribution Pattern of the Knee: A Study of Normal and Osteoarthrotic Knee Joints. Acta Orthop Scand 51:871–879
8. King TV, Vallee BL (1991) Neovascularization of the meniscus with angiogenin. An experimental study in rabbits. J Bone Joint Surg 73(4):587–590
9. Lohmander LS, Englund PM, Dahl LL, Roos EM (2007) The Long-term Consequence of Anterior Cruciate Ligament and Meniscus Injuries. Am J Sports Med 35:1756–1769
10. Webber RJ (1990) In vitro culture of meniscal tissue. Clin Orthop Relat Res 252:114–117
11. Landa SC et al (2012) Efecto de la sobreexpresión de angiogenina sobre células aisladas del menisco humano. Investig Discapac 1(2):53–58
12. Sun Y et al (2010) Analysis of meniscal degeneration and meniscal gene expression. BMC Musculoskelet Disord 11:19
13. Goldring SR, Goldring MB (2016) Changes in the osteochondral unit during osteoarthritis: structure, function and cartilage–bone crosstalk. Nat Rev Rheumatol 12:632–644
14. Martel-Pelletier J et al (2016) Osteoarthritis. Nat Rev Dis Primers 2:16072
15. Chen S, Fu P, Wu H, Pei M (2017) Meniscus, articular cartilage and nucleus pulposus: a comparative review of cartilage-like tissues in anatomy, development and function. Cell Tissue Res 370:53–70
16. Santangelo KS, Nuovo GJ, Bertone AL (2012) In vivo reduction or blockade of interleukin-1β in primary osteoarthritis influences expression of mediators implicated in pathogenesis. Osteoarthritis Cartilage 20:1610–1618
17. Kumar A, Takada Y, Boriek AM, Aggarwal BB (2004) Nuclear factor-κB: its role in health and disease. J Mol Med 82:434–448
18. Li Z et al (2017) Omentin-1 prevents cartilage matrix destruction by regulating matrix metalloproteinases. Biomed Pharmacother 92:265–269
19. Wang M et al (2011) Recent progress in understanding molecular mechanisms of cartilage degeneration during osteoarthritis. Ann NY Acad Sci 1240:61–69
20. Fioravanti A et al (2012) In Vitro Effects of VA441, a New Selective Cyclooxygenase-2 Inhibitor, on Human Osteoarthritic Chondrocytes exposed to IL-1β. J Pharmacol Sci 120:6–14
21. Tchetina EV (2011) Developmental Mechanisms in Articular Cartilage Degradation in Osteoarthritis. Arthritis 2011:1–16
22. Zindel J, Kubes P (2020) DAMPs, PAMPs, and LAMPs in Immunity and Sterile Inflammation. Annu Rev Pathol Mech Dis 15:493–518
23. Jiang Z et al (2021) Whole-Transcriptome Sequence of Degenerative Meniscus Cells Unveiling Diagnostic Markers and Therapeutic Targets for Osteoarthritis. Front Genet 12:654321
24. McNulty AL, Rothfusz NE, Leddy HA, Guilak F (2013) Synovial fluid concentrations and relative potency of interleukin-1 alpha and beta in cartilage and meniscus degradation. J Orthop Res 31:1039–1045
25. Cook A, Cook J, Stoker A (2018) Metabolic Responses of Meniscus to IL-1β. J Knee Surg 31:834–840
26. Fu W et al (2022) Cellular features of localized microenvironments in human meniscal degeneration: a single-cell transcriptomic study. eLife 11:e78385
27. Salazar JR et al (2011) Determinación del mecanismo anti-inflamatorio de peniocerol y chichipegenina aislados de Myrtillocactus geometrizans. Rev Mex Cienc Farm 42(3):45–53
28. Salazar JR et al (2020) Chemistry, Biological Activities and In Silico Bioprospection of Sterols and Triterpenes from Mexican Columnar Cactaceae. Molecules 25(7):1649
29. Couder-García BDC et al (2019) The Phytosterol Peniocerol Inhibits Cell Proliferation and Tumor Growth in a Colon Cancer Xenograft Model. Front Oncol 9:1341
30. Röthlisberger C, Dettwiler A, Gaille GG, Zuppinger A (1971) Studies on calcium metabolism in humans with the aid of a whole body counter. Whole body retention of Ca47 in the healthy and in patients with tumors and other diseases. Radiol Clin Biol 40:200–211
31. Trachootham D, Alexandre J, Huang P (2009) Targeting cancer cells by ROS-mediated mechanisms: a radical therapeutic approach? Nat Rev Drug Discov 8:579–591
32. Warburg O, Wind F, Negelein E (1927) The Metabolism of Tumors in the Body. J Gen Physiol 8:519–530
33. Long Y et al (2019) Substantive molecular and histological changes within the meniscus with tears. BMC Musculoskelet Disord 20:577
34. Qi Y, Tang R, Shi Z, Feng G, Zhang W (2021) Wnt5a/Platelet-rich plasma synergistically inhibits IL-1β-induced inflammatory activity through NF-κB signaling pathway and prevents cartilage damage and promotes meniscus regeneration. J Tissue Eng Regen Med 15:612–624
35. Jacob G, Shimomura K, Krych AJ, Nakamura N (2019) The Meniscus Tear: A Review of Stem Cell Therapies. Cells 9:92
36. Choi M-C, Jo J, Park J, Kang HK, Park Y (2019) NF-κB Signal-

ing Pathways in Osteoarthritic Cartilage Destruction. Cells 8:734
37. Zhu L et al (2025) Liposomic lubricants suppress acute inflammatory gene regulation in the joint in vivo. Acta Biomater 198:366–376
38. Martinez-Armenta C et al (2021) Therapeutic Potential of Bioactive Compounds in Honey for Treating Osteoarthritis. Front Pharmacol 12:723618
39. Lee YT, Yunus MHM, Ugusman A, Yazid MD (2022) Natural Compounds Affecting Inflammatory Pathways of Osteoarthritis. Antioxidants 11:1722
40. Lei M et al (2012) Resveratrol inhibits interleukin 1β-mediated inducible nitric oxide synthase expression in articular chondrocytes by activating SIRT1 and thereby suppressing nuclear factor-κB activity. Eur J Pharmacol 674:73–79
41. Liu L et al (2014) Protective Effect of Resveratrol against IL-1β-Induced Inflammatory Response on Human Osteoarthritic Chondrocytes Partly via the TLR4/MyD88/NF-κB Signaling Pathway: An "in Vitro Study". Int J Mol Sci 15:6925–6940
42. Zhang C et al (2018) Chrysin protects human osteoarthritis chondrocytes by inhibiting inflammatory mediator expression via HMGB1 suppression. Mol Med Rep 18:3622–3629
43. Zheng W et al (2017) Chrysin Attenuates IL-1β-Induced Expression of Inflammatory Mediators by Suppressing NF-κB in Human Osteoarthritis Chondrocytes. Inflammation 40:1143–1154